JOC The Journal of Organic Chemistry

Article

pubs.acs.org/joc

"Planetary Orbit" Systems Composed of Cycloparaphenylenes

Steven M. Bachrach* and Zeina-Christina Zayat

Department of Chemistry, Trinity University, One Trinity Place, San Antonio, Texas 78212, United States

Supporting Information

ABSTRACT: Cycloparaphenylenes (CPP) can serve as both guest and host in a complex. Geometric analysis indicates that optimal binding occurs when the CPP nanohoops differ by five phenyl rings. Employing C-PCM(THF)/ωB97X-D/6-31G(d) computations, we find that the strongest binding does occur when the host and guest differ by five phenyl rings. The guest CPP is modestly inclined relative to the plane of the host CPP except when the host and guest differ by four phenyl rings, when the inclination angle becomes >40°. The distortion/interaction model shows that interaction dominates and is best when the host and guest differ by five phenyl rings. The computed ^{1}H NMR shifts of the guest CPP are shifted by about 1 ppm upfield relative to their position when unbound. This distinct chemical shift should aid in experimental detection of these CPP planetary orbit complexes.

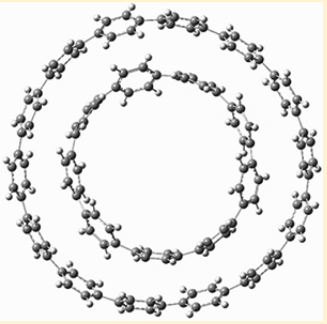

INTRODUCTION

Cycloparaphenylenes (CPP, see Scheme 1) are of interest to organic chemists for a variety of reasons.[1] Their structures allow for playing the effects of aromaticity off of strain.[2−5] Their curved π-surfaces may produce interesting electro-optical properties.[6] Their curved interior space makes them suitable hosts for guest molecules with complementarily curved surfaces, such as the fullerenes.[7,8] The CPPs might serve as a template from which to build nanostructures such as nanotubes.[9,10] Lastly, their structures pose a significant synthetic challenge. This past decade has seen a "golden age" in the synthesis of CPPs, as selective methods for preparing a wide range of CPPs have been discovered.[1,6,11] While the medium-sized CPPs were the first to be prepared, such as [8]-,[12] [9]-,[13] and [12]CPP,[13] even the highly strained [5]CPP[14,15] and [6]CPP[16,17] molecules have now been synthesized.

Scheme 1

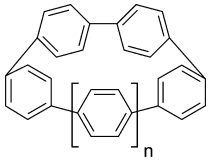

CPP, for example, n=4: [8]CPP

The synthesis of the CPPs has led to multiple studies of the interesting properties and features of these curved systems. A variety of host−guest complexes with the CPP molecule serving as the host have been identified, both synthetically and computationally.[7,8,18−22] Perhaps most iconic are the so-called "Saturn systems",[22] where a fullerene (standing in for the planet Saturn) is surrounded by a CPP (representing the rings about Saturn). An example of a "Saturn system" is shown in Figure 1; this is the complex of [10]CPP with a C_{60}-fullerene inside (also denoted as [10]CPP⊃C_{60}).[7]

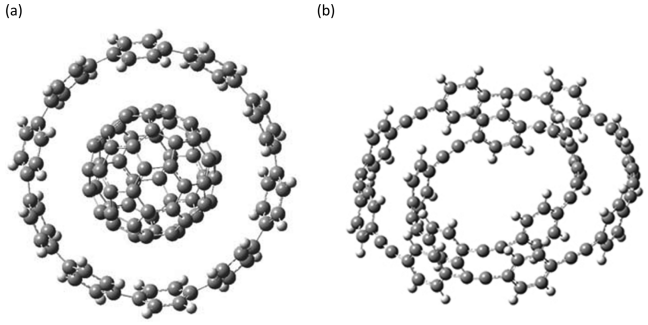

Figure 1. Structures of (a) [10]CPP⊃C_{60} and (b) [8]CPPA:[5]CPPA.

In 2012, Fomine, Zolotukhin, and Guadarrama conjectured that a larger CPP nanohoop might act as host for a smaller CPP nanohoop.[21] In fact, they suggested that one might be able to nest a series of ever smaller nanohoops inside one another, creating what they termed a "Russian doll" complex. Assuming that the ideal distance between the nanohoops would be 3.5 Å, geometric analysis led to the prediction that two nested CPP nanohoops would differ by five phenyl rings. Limited testing of this hypothesis at M06-2X/6-31G* found that the binding energy of the [14]:[9] complex was greater than either the [13]:[9] or [15]:[9] complex. Their computed structure of the [14]:[9] complex is shown, in top and side view, in Figure 2. Alvarez et al. created a 1:1 mixture of [6]CPP and [12]CPP and subjected it to pressure.[23] They observed little spectral change, unlike when [6]CPP alone was subjected to pressure. They suggest that the larger nanohoop acts as a "pressure protector" of the smaller internally held nanohoop.

The related cycloparaphenylacetylene (CPPA) nanohoops have also been investigated. Kawase and colleagues have

Received: February 15, 2016
Published: May 10, 2016

DOI: 10.1021/acs.joc.6b00339
J. Org. Chem. 2016, 81, 4559−4565

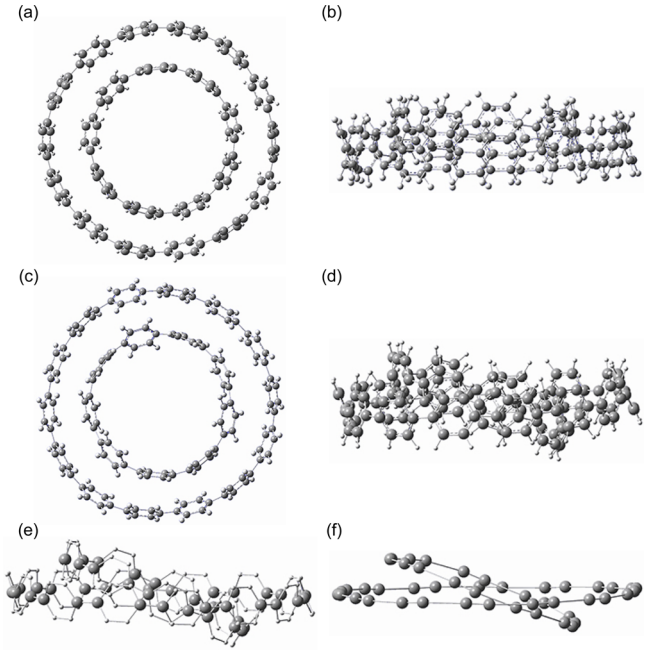

Figure 2. Structure of the [14]:[9] complex. Reported by Fomine et al.:[21] (a) top and (b) side view. Optimized at CPCM(THF)/ωB97X-D/6-31G(d): (c) top and (d) side view. (e) Structure with hydrogens suppressed and emphasizing the *ipso* carbons. (f) ellipse-like shape constructed by joining the *ipso* carbons.

prepared a number of CPPA nanohoops and have identified some nanohoop clusters.[24] For example, the [8]CPPA:[5]CPPA cluster (shown in Figure 1) has a binding free energy of −5.51 kcal mol^{-1}.

In this study, we provide a broader computational exploration of the embedded nanohoop complex, surveying many of the possibilities involving [6]CPP to [16]CPP. We utilize a density functional (ωB97X-D) that explicitly corrects for dispersion. The binding free energies are examined using the distortion/interaction model.[25,26] Computed NMR chemical shifts are provided to assist in the identification of these complexes.

COMPUTATIONAL METHODS

All computations were performed with the *Gaussian 09* suite.[27] The structures of the cycloparaphenylene nanohoops were optimized at ωB97X-D/6-31G(d),[28] a density functional that accounts for dispersion. These geometries were then used to create the specific nanohoop complexes, designated as [***m***]:[***n***], where ***m*** and ***n*** designate the number of phenyl rings within each nanohoop, with ***m*** > ***n***. A number of different configurations of some of the complexes were located, but in general the structures obtained are representative of the complex geometry and not necessarily the global minimum energy structure. All complexes were identified as being local energy minima by finding only real vibrational frequencies.

The nanohoop complexes were then reoptimized using the conductor polarized continuum method (C-PCM)[29] modeling THF as solvent with the same computational method as mentioned above. Analytical frequencies were recomputed as well. The unscaled zero-point vibrational frequencies were utilized in computing enthalpy and free energies, incorporating the quasiharmonic approximation of Truhlar and Cramer whereby low-frequency modes (less than 100 cm^{-1}) were raised to 100 cm^{-1} for the computation of the vibrational partition functions.[30] We report here the solution-phase enthalpies and free energies evaluated at 25 °C and 1 atm, while the gas phase results are included in the Supporting Information.

NMR chemical shifts were computed at CPCM(THF)/B3LYP/6-31G(d)[31] with the CPCM(THF)/ωB97X-D/6-31G(d) geometries, due to the inability of the program to compute the chemical shifts with the ωB97X-D functional. The ^{1}H and ^{13}C chemical shifts are reported without scaling.

RESULTS

[14]:[9] Complex. Fomine and co-workers reported the gas-phase structure of the [**14**]:[**9**] complex at M06-2X/6-31G*.[21] As seen in Figure 2a, the smaller [9]CPP hoop is situatued inside the larger nanohoop, but viewing this complex from the side (Figure 2b) reveals that the smaller [9]CPP ring lies above the equatorial plane of the larger [14]CPP nanohoop. We reoptimized the structure of [**14**]:[**9**] at ωB97X-D/6-31G(d) starting with the two rings lying in each others equatorial plane; this led to the structure shown in Figure 2c and 2d. In this structure, the [9]CPP lies at an angle to the larger hoop. To get a sense of arrangement, we have emphasized the *ipso* carbons of each phenyl ring, suppressing the hydrogens in Figure 2e. Then, by connecting the adjacent *ipso* carbons, we create an ellipse-like ring for each of the nanohoops (Figure 2f). These ellipse-like rings can be a least-squares fit to a plane, defining the equatorial plane, and the angle between these planes, called the inclination, can be computed. These ellipse-like rings are reminiscent of the planetary orbits about the sun, and the angles between their planes are analogous to the inclination of planetary orbits.

The M06-2X/6-31G* optimized structure of the [**14**]:[**9**] complex in the inclined ("planetary orbit", Figure 2c) configuration is 2.45 kcal mol^{-1} lower in free energy than the displaced ("Russian doll", Figure 2a) structure. The "planetary orbit" configuration is favored over the "Russian doll" one by 1.27 kcal mol^{-1} at ωB97X-D/6-31G(d). A sampling of some of the other CPP complexes also finds the "planetary orbit" configuration to be preferred over the "Russian doll" configuration. All of the CPP complexes discussed hereafter are in the "planetary orbit" configuration.

Geometries of the CPP Complexes. A representative sample of the solution-phase (CPCM(THF)/ωB97X-D/6-31G(d)) CPP complexes are shown in Figure 3, where the larger nanohoop host is [14]CPP and the guest nanohoop ranges from [6]- to [10]CPP. Images of the other complexes are shown in the Supporting Information. In general, the gas phase and solution phase structures are quite similar, as are their binding energies. For that reason, we discuss here only the solution phase results for better comparison with experimental conditions. The gas phase results are included in the Supporting Information.

Some interesting trends can be observed in this series. First, while all of the smaller CPP rings are situated in the interior of the larger host nanohoop, the guest is not necessarily in the center of the host. As seen in the [**14**]:[**6**] complex, the smaller nanohoop is positioned well-off to one side of the guest. If we take the geometric average of the positions of the *ipso* carbons in each CPP nanohoop as representative of its center, then the hoop centers are 2.75 Å apart. Inspection of both Figure 3 and Table 1 shows that, for the series of complexes with [14]CPP as the host, the guest moves closer and closer to the center of the host with increasing size of guest. The more general trend, seen with [12]-, [13]-, and [16]CPP as hosts, is that the distances between the hoop centers decreases with increasing guest size until it reaches a minimum, and then the centers become farther apart with larger guest size. This trend is also

DOI: 10.1021/acs.joc.6b00339
J. Org. Chem. 2016, 81, 4559−4565

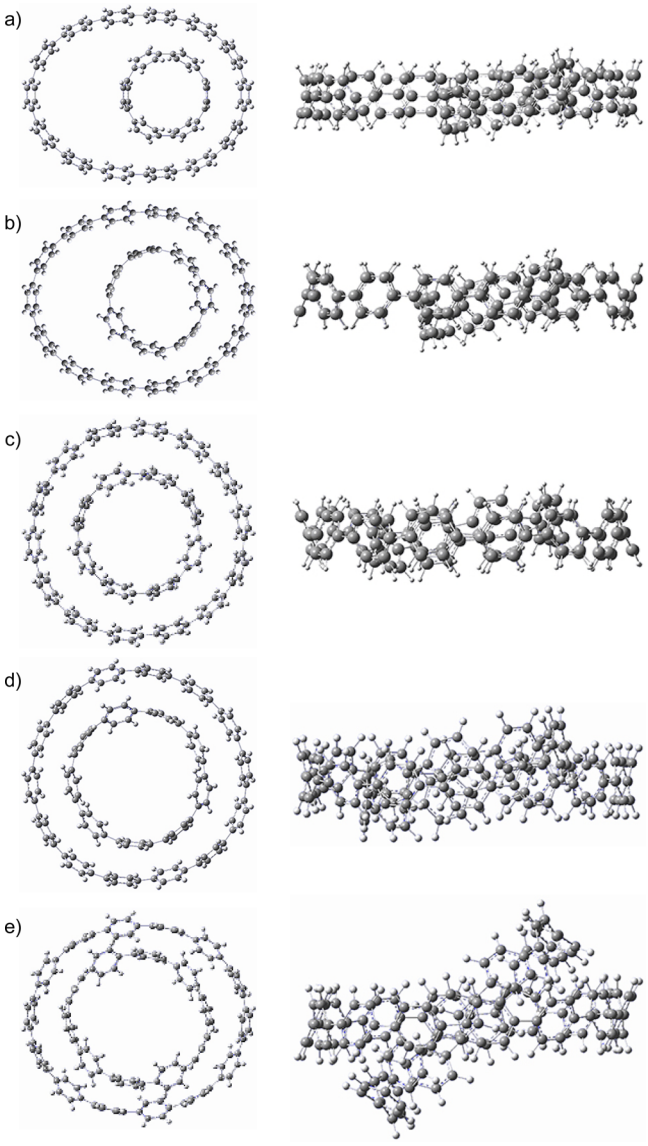

Figure 3. Top and side views of the ωB97X-D/6-31G(d) optimized geometries of (a) [**14**]:[**6**], (b) [**14**]:[**7**], (c) [**14**]:[**8**], (d) [**14**]:[**9**], (e) [**14**]:[**10**].

Table 1. Distance (Å) between the Centers of the Two Nanohoops within a Complex

	smaller nanohoop					
larger nanohoop	6	7	8	9	10	11
10	0.00					
11	0.21					
12	0.28	0.01	1.75			
13	1.61	0.34	0.51	2.08		
14	2.75	1.70	0.12	0.30	0.00	
15					0.28	
16	4.77		2.87			0.31

seen in the series where the guest is held fixed, say [8]CPP, and the host size is varied.

All of the isolated CPPs have high axial symmetry, indicating a circle-like appearance. While the nanohoops in the [**14**]:[**8**] and [**14**]:[**9**] complexes look fairly circular, the same is not true for the host nanohoop in the [**14**]:[**6**] and [**14**]:[**7**] complexes; the [14]CPP has a decided ellipsoid shape in these complexes. This type of distortion can be measured as flattening, defined as $1 - b/a$, where a is the distance of the across the larger axis and b is the distance across the shorter axis (see Scheme S1 for further definition). Table 2 lists the degree of flattening of each nanohoop in each complex.

Table 2. Flattening of Each Nanohoop within a Complex[a]

	smaller nanohoop					
larger nanohoop	6	7	8	9	10	11
10	0.106					
	0.083					
11	0.034					
	0.069					
12	0.006	0.010	0.091			
	0.004	0.024	0.082			
13	0.195	0.022	0.050	0.093		
	0.002	0.005	0.014	0.094		
14	0.253	0.183	0.011	0.013	0.128	
	0.003	0.040	0.012	0.045	0.087	
15					0.021	
					0.052	
16	0.296		0.255		0.024	0.025
	0.007		0.013			0.064

[a]Larger ring first entry, smaller ring second entry.

For most of these complexes, the flattening of the host is greater than the flattening of the guest. The flattening is most pronounced when the sizes of the host and guest are dramatically different, particularly when they differ by seven or more phenyl rings; the largest distortion is of [16]CPP in the [**16**]:[**6**] complex. As the difference in the number of phenyl rings decreases from 7, the distortions diminish to a minimum where the difference in the number of phenyl rings is about 5, but a difference of 4 phenyl rings results in greater flattenings.

As readily seen in the side views of the complexes shown in Figure 3, the two nanohoops are inclined with respect to each other. The angle of inclination between the two planes that best fit the coordinates of the *ipso* carbons in each hoop of the complex are listed in Table 3. The largest inclination angles are

Table 3. Inclination (deg) of the Two Nanohoops within a Complex

	smaller nanohoop					
larger nanohoop	6	7	8	9	10	11
10	48.7					
11	34.2					
12	6.2	28.5	44.1			
13	9.3	16.0	26.3	37.0		
14	8.8	15.1	10.0	20.3	41.7	
15					17.3	
16	13.0		14.6			15.0

for the complexes where the host and guest differ by four phenyl groups, such as [**12**]:[**8**] where the inclination angle is 44.1°. There are no other decisive trends in the inclination angles.

Binding Energies. The binding enthalpy and free energy for the formation of each CPP complex are listed in Table 4.

DOI: 10.1021/acs.joc.6b00339
J. Org. Chem. 2016, 81, 4559−4565

Table 4. Binding Enthalpy and Free Energy for the Complexes of Two Nanohoops[a]

	smaller nanohoop					
larger nanohoop	6	7	8	9	10	11
10	−29.52					
	−10.24					
11	**−43.06**					
	−25.58					
12	−39.23	**−46.62**	−39.15			
	−17.02	***−28.33***	*−21.76*			
13	−29.19	−42.08	**−50.89**	−45.08		
	−10.57	*−22.07*	***−29.56***	*−25.01*		
14	−24.48	−32.16	−46.53	**−52.92**	−44.28	
	−7.53	*−13.42*	*−29.22*	***−32.13***	*−24.77*	
15					**−58.34**	
					−38.02	
16	−20.96		−33.39			**−63.69**
	−2.22		*−13.26*			***−40.02***

[a]In kcal mol^{-1}. Binding enthalpy in plain face, binding free energy in italics. Energies in bold face indicate the strongest binding within a series.

These data confirm the prediction of Fomine et al.[21] that the strongest interaction will be for the CPP pair that differ by five phenyl groups. So, for example, in the series of complexes with [14]CPP as host, the binding becomes stronger (both the enthalpy and free energy becomes more negative) when the guest increases in size from [6]- to [9]-CPP, and then gets weaker with [10]CPP. Similarly, for the series with [8]CPP as the guest, the [**13**]:[**8**] complexes have the strongest binding enthalpy and free energy. The binding enthalpy and free energy are smaller for [**12**]:[**8**], and they both decrease with increasingly larger hosts as well.

These computed binding enthalpies can be quite large, upward of −60 kcal mol^{-1}. Even the binding free energies are predicted to be quite large, up to −40 kcal mol^{-1}.

Some comparison to experimental values would be useful for benchmarking these computed enthalpies. Since no experimental binding energies are known for the CPP clusters, we need to compare some analogue systems, namely the binding free energies of [10]CPP⊃C_{60}, [8]CPPA:[5]CPPA, and [9]CPPA:[6]CPPA. The CPCM(THF)/ωB97X-D/6-31G(d) binding free energy of [10]CPP⊃C_{60} is −37.2 kcal mol^{-1}, significantly more than the experimental value of −9.1 kcal mol^{-1}.[7] Similar overestimation of the binding energies of [8]CPPA:[5]CPPA and [9]CPPA:[6]CPPA are found; the binding free energies are overestimated by 19.1 and 26.9 kcal mol^{-1}, respectively.

Grimme[32] has described a computational method that affords very respectable binding free energies for a range of host−guest complexes. The procedure involves using a triple-ζ def2-TZVP basis set, using the D3 dispersion correction, the HF-3c method for correcting vibrational frequencies, and the COSMO-RS method for accounting for solvation. Unfortunately our computational resources are insufficient to perform these large computations of the nanohoop complexes examined here.

However, Rehman, McKee, and McKee[22] reported the binding free energy of [10]CPP⊃C_{60} in dichloromethane using M05-2X/6-31G(d) and the SMD[33] procedure to account for the effects of solvation. This computed value of −12.8 kcal mol^{-1} only overestimates the binding free energy by 3.7 kcal mol^{-1}. We therefore calculated the binding free energies of the model systems at SMD(THF)/ωB97X-D/6-31G(d) using the CPCM(THF)/ωB97X-D/6-31G(d) geometries, and these energies are listed in Table 5. The SMD energies are 10−12 kcal mol^{-1} closer to the experimental values, though they still overestimate the binding energy.

Table 5. Binding Free Energies (kcal mol^{-1}) for Model Systems

model	CPCM[a]	SMD[b]	expt
[10]CPP⊃C_{60}	−37.19	−25.57	−9.1
[8]CPPA:[5]CPPA	−24.63	−11.11	−5.5
[9]CPPA:[6]CPPA	−29.13	−19.77	−2.2

[a]Computed at CPCM(THF)/ωB97X-D/6-31G(d). [b]Computed at SMD(THF)/ωB97X-D/6-31G(d) using the CPCM(THF)/ωB97X-D/6-31G(d) geometries.

We recomputed the binding enthalpy at free energies using the SMD procedure for many of the nanohoop complexes, and these values are listed in Table S2. The binding free energies are reduced by 10−15 kcal mol^{-1}, but are likely still too large, based on the computations of the model systems (Table 5). When a correction of 10−15 kcal mol^{-1} is applied to these SMD free energies, the resulting binding energies are at best negative by about 5 kcal mol^{-1}.

Distortion/Interaction Energies. Houk offered the distortion/interaction model as a means for parsing energetic interactions.[25,26] For each complex, the energy of each nanohoop is computed separately in its geometry in the complex; the difference in the energy of this distorted nanohoop and its optimized energy is the distortion energy. The binding energy less the distortion energy is the interaction energy. (See Scheme S2 for a detailed example of this computation.) The distortion and interactions energies for the CPP complexes are listed in Table 6.

For all of the complexes except [**16**]:[**11**], the distortion energy of the larger CPP, the host, is bigger than the distortion energy of the smaller CPP, the guest. The distortion energy of the guest CPPs range from about 0.2 (for [6]CPP in [**12**]:[**6**]) to 2.7 kcal mol^{-1} (for [11]CPP in [**16**]:[**11**]), and for the host CPPs it ranges from 0.6 (for [12]CPP in [**12**]:[**6**]) to 10.1 kcal mol^{-1} (for [10]CPP in [**10**]:[**6**]). The total distortion energy ranges from 0.8 (for [**12**]:[**6**]) to 12.1 kcal mol^{-1} (for [**10**]:[**6**]).

In looking at the distortion energy for a series of complexes, keeping either the host or guest size fixed and increasing the

DOI: 10.1021/acs.joc.6b00339
J. Org. Chem. 2016, 81, 4559−4565

Table 6. Distortion and Interaction Energies (kcal mol^{-1}) for the Complexes of Two Nanohoops[a]

	smaller nanohoop					
larger nanohoop	6	7	8	9	10	11
10	12.08					
	−43.90					
11	1.38					
	−45.72					
12	0.79	1.83	4.61			
	−39.61	−50.34	−46.09			
13	4.61	1.47	1.83	2.94		
	−33.55	−44.39	−54.41	−51.19		
14	5.31	2.81	1.73	3.75	4.57	
	−31.78	−36.93	−49.69	−59.53	−51.82	
15					4.84	
					−65.09	
16	6.27		4.39			5.30
	−28.44		−38.83			−70.66

[a]Distortion energy first entry, interaction energy second entry.

size of the other CPP, we again see the trend of going through a minimum. For example, with [6]CPP as the guest, the distortion energy decreases when the host increases from [10]- to [12]CPP, but then it increases as the host becomes larger. Unlike with the binding energy, where the strongest binding occurs when the host and guest differ by five phenyl units, the distortion energy is at a minimum when the host and guest differ by six phenyl units.

A similar trend is also observed with the interaction energy. If we look at the complexes with [14]CPP as the host, the interaction energy steadily become more negative as the size of the guest goes from 6 to 9 phenyl rings, and then increases with [10]CPP. The strongest interaction energy is found when the host and guest nanohoops differ by five phenyl rings. These trends in binding enthalpy, distortion energy, and interaction energy can be seen in Figure 4, where we display these values for [14]CPP as the host.

NMR Chemical Shifts. The ^{1}H and ^{13}C NMR chemical shifts of the CPPs were computed and compared to experimental[5] values. The proton chemical shifts were averaged, as are the chemical shifts of the *ipso*-carbons and the other carbons. This averaging process helps to account for some of the dynamics of the CPP hoops that leads to the equivalencing of the protons that point to the interior of the ring with those that point to the exterior of the nanohoop. The experimental ^{1}H NMR shows a single signal indicating the rapid dynamics that average all of the protons.

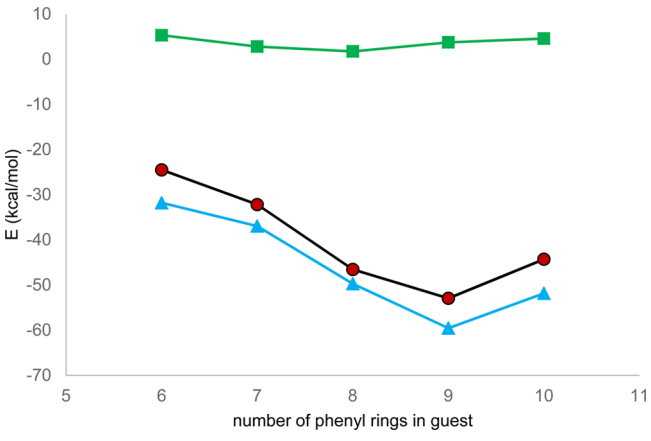

Figure 4. Variation of the binding enthalpy (black circles), distortion energy (green squares), and interaction energy (blue triangles) for different CPP guest with [14]CPP as the host.

Both the computed proton and carbon chemical shifts of the CPPs are too small and can be scaled to fit the experimental values quite nicely (see the Supporting Information for details). The ^{1}H chemical shifts increase with increasing size of the nanohoop, from about 7.5 to 7.7 ppm. The experimental ^{1}H chemical shift of [6]CPP of 7.64 ppm[16] appears to be too high. The chemical shift of the *ipso* carbons are around 138 ppm and the other carbons appear around 127 ppm, with no discernible trend with varying the size of the nanohoop.

These scaling factors were then applied to the computed ^{1}H and ^{13}C chemical shifts of the complexes and are reported in Table 7 and Table S5. Two major trends can be identified. The proton chemical shift of the larger CPP ring in the complex are in general little affected by the guest. On the other hand, the proton chemical shifts of the guest CPP are shifted to smaller values, ranging from 6.2 to 6.9 ppm. The ^{13}C chemical shifts of the complex are little changed relative to the individual CPP molecules (see Table S5).

Table 7. Computed ^{1}H NMR Chemical Shifts (ppm) for the Complexes of Two Nanohoops[a]

	smaller nanohoop					
larger nanohoop	6	7	8	9	10	11
11	7.59					
	6.19					
12	7.41	7.57	7.73			
	6.43	6.35	6.63			
13	7.46	7.49	7.59	7.66		
	6.53	6.46	6.40	6.80		
14	7.49	7.51	7.50	7.55		
	6.61	6.58	6.50	6.46		
15					7.56	
					6.51	
16	7.54		7.55			7.53
	6.72		6.64			6.69

[a]For each complex, the chemical shifts for the larger hoop are on top and those for the smaller hoop on bottom.

DOI: 10.1021/acs.joc.6b00339
J. Org. Chem. 2016, 81, 4559−4565

It should be noted that these computed chemical shifts are for a single configuration of the CPP complexes. Averaging the chemical shifts of the protons in each nanohoop should account for some motions, such as the twisting within a hoop that passes one phenyl by a neighboring phenyl and rotation of the entire hoop about an axis perpendicular to the nanohoop. The principal motion that is not accounted for changes the inclination angle of one nanohoop relative to the either. However, as long as the guest remains within the interior of the host, our general result should hold: that the proton chemical shift of the guest is shifted upfield relative to that in its unbound state.

DISCUSSION

Fomine and co-workers[21] suggested that optimal binding between two CPP nanohoops would occur when the hoops differ by 3.5 Å, which by geometric arguments corresponds to a difference of five phenyl rings. Figure 5 displays the radius of

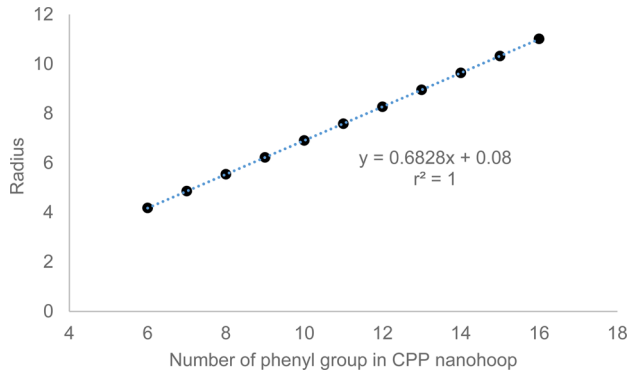

Figure 5. Plot of the radius (Å) of the CPP nanohoops against the number of phenyl rings.

the CPP nanohoops with 6 to 16 phenyl rings. The excellent linear fit suggests that a separation of 3.5 Å would occur with nanohoops differing by 5.12 phenyl rings. A difference of five phenyl rings between two nanohoops projects into a physical separation of 3.41 Å. This is just slightly larger than the separation of 3.37 Å found between the rings in the slipped parallel C_{2h} benzene dimer (at ωB97X-D/6-31G(d)). However, since adjacent phenyl rings in the CPP nanohoops alternate back-and-forth to minimize the $o-o'$-hydrogen interactions, the phenyl rings of the guest nanohoop protrude into its interior reducing the size of the cavity. Nonetheless, the strongest binding is found in the complexes where the host contains five more phenyl rings than the guest. Two distinct geometric changes are the result of this binding: the host and the guest distort from a circular shape and the planes of the two nanohoops are at an angle to each other.

The geometric distortions are diagramed in Scheme 2. The host distorts to create a slightly larger cavity in the plane of the guest (black arrow pushing outward) while the guest compresses in the plane of the host (the blue arrow pushing inward). The guest resides in a plane inclined to the plane of the host, thereby minimizing steric interactions (the red arrows). For these [*m*]:[*m*-5] complexes, the distortion energies are small: less than 2 kcal mol^{-1} for the complexes with m = 11, 12, or 13, and increasing to 5.3 kcal mol^{-1} with m = 16. The smaller CPP rings are more costly to distort, because they are already so strained. Therefore, these smaller complexes tend to suffer from lesser distortion energy. The complexes,

Scheme 2. Distortions of the CPPs in a Complex (See Text for Discussion)

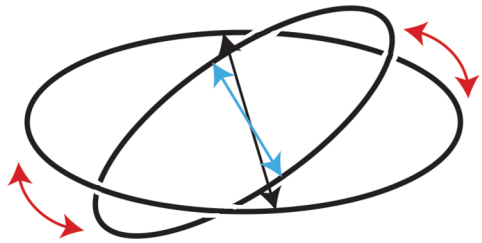

though, benefit from increasing interaction energy as the CPP rings increase in size; this results from a greater contact area between the host and guest in these larger complexes leading to greater dispersion energy.

When the difference in the number of phenyl groups within the host and guest is four, the distortions are more severe. The guest compresses further and the host expands, but the constraints of the ring, especially the desire for each phenyl ring to be planar, limit how much distortion can be done. The major adjustment is for the inclination of the ring planes to dramatically increase, to values over 40° in all cases examined. In addition, the centers of each ring separate to move the width of the interior ring (see the blue arrow in Scheme 2) out of the plane of the host molecule. This large inclination and separation of the ring centers minimizes the steric clashes of the CPP rings, but comes with decreased contact between host and guest and consequently lesser interaction energy. For example, the distortion energy of [**14**]:[**10**] is 4.57 kcal mol^{-1}, only 0.82 kcal mol^{-1} larger than the distortion energy of [**14**]:[**9**]. However, since the inclination angle is so much greater in [**14**]:[**10**] (41.7°) than in [**14**]:[**9**] (20.3°), the interaction energy of 51.82 kcal mol^{-1} of [**14**]:[**10**] is 7.71 kcal mol^{-1} less than that of [**14**]:[**9**].

For the complexes where the host is made up of five or more phenyl rings than the guest, then if the two CPP rings are concentric, the distance between any phenyl on the host would be farther than optimal to any phenyl in the guest. To bring at least some phenyl rings of the host and guest near each other, the guest must shift to one side of the host, as observed by the large distance between the center of the two nanohoops (Table 1), and the host will distort by wrapping around the guest in an attempt to bring as many phenyl rings into contact between the two CPPs. This is readily observed in the [**14**]:[**6**] complex shown in Figure 3a.

The fact that the binding enthalpies and free energies are overestimated by the DFT and solvation methods applied here limits what can be said concerning the possibility of these nanohoop complexes being formed. Applying a correction of 10−15 kcal mol^{-1} to the SMD free energies suggests that the binding free energies for most of the complexes will be at best a handful of kcal mol^{-1}, and undoubtedly some of them will have positive binding energies. This does agree with the fact that there is only one indirect report of an observation of a nanohoop complex.[23] However, the computations do suggest that any future endeavors to identify a nanohoop complex focus on those where the hoop sizes differ by five phenyl rings.

CONCLUSIONS

A smaller cycloparaphenylene nanohoop can bind to the interior of a larger cycloparaphenylene nanohoop. The

DOI: 10.1021/acs.joc.6b00339
J. Org. Chem. 2016, 81, 4559−4565

strongest binding complexes occur when the rings differ by five in their number of phenyl groups.

Due to the *o*−*o*′-hydrogen interactions, the phenyl rings in the CPPs alternate, diminishing the interior space of the nanohoops. The guest CPP inclines from the host CPP, forming what we term "planetary orbit" systems. The inclination angle is modest for complexes where the host CPP possesses five or more phenyl rings than the guest. When the difference is only four phenyl rings, the interior of the host is too confined to accommodate the guest, and the inclination angle is large, over 40°.

The computed ^{1}H NMR chemical shifts of the planetary orbit CPP complexes suggest a rather large upfield shift for the protons of the guest CPP. These protons should appear at 6.5 to 6.7 ppm, about 1 ppm below the usual chemical shift for unbound CPP systems. We hope that these predictions might guide the experimental observation of CPP planetary orbit complexes.

■ ASSOCIATED CONTENT

Supporting Information

The Supporting Information is available free of charge on the ACS Publications website at DOI: 10.1021/acs.joc.6b00339.

Full listing of ref 27, images of all complexes, gas phase and SMD binding enthalpies and free energies, scaling factors for NMR chemical shifts, computed ^{13}C NMR chemical shifts, and coordinates of all CPPs and complexes (PDF)

■ AUTHOR INFORMATION

Corresponding Author

*E-mail: sbachrach@trinity.edu.

Notes

The authors declare no competing financial interest.

■ ACKNOWLEDGMENTS

The authors thank the Robert A. Welch Foundation (Grant W-0031) and Trinity University for support of this project. We thank Prof. Chris Cramer and Will Isley for a script to perform the quasiharmonic approximation and the reviewers of this paper for helpful comments.

■ REFERENCES

(1) Lewis, S. E. *Chem. Soc. Rev.* **2015**, *44*, 2221−2304.
(2) Wong, B. M. *J. Phys. Chem. C* **2009**, *113*, 21921−21927.
(3) Segawa, Y.; Omachi, H.; Itami, K. *Org. Lett.* **2010**, *12*, 2262−2265.
(4) Bachrach, S. M.; Stück, D. *J. Org. Chem.* **2010**, *75*, 6595−6604.
(5) Iwamoto, T.; Watanabe, Y.; Sakamoto, Y.; Suzuki, T.; Yamago, S. *J. Am. Chem. Soc.* **2011**, *133*, 8354−8361.
(6) Golder, M. R.; Jasti, R. *Acc. Chem. Res.* **2015**, *48*, 557−566.
(7) Iwamoto, T.; Watanabe, Y.; Sadahiro, T.; Haino, T.; Yamago, S. *Angew. Chem., Int. Ed.* **2011**, *50*, 8342−8344.
(8) Iwamoto, T.; Watanabe, Y.; Takaya, H.; Haino, T.; Yasuda, N.; Yamago, S. *Chem. - Eur. J.* **2013**, *19*, 14061−14068.
(9) Omachi, H.; Nakayama, T.; Takahashi, E.; Segawa, Y.; Itami, K. *Nat. Chem.* **2013**, *5*, 572−576.
(10) Page, A. J.; Ding, F.; Irle, S.; Morokuma, K. *Rep. Prog. Phys.* **2015**, *78*, 036501.
(11) Hirst, E. S.; Jasti, R. *J. Org. Chem.* **2012**, *77*, 10473−10478.
(12) Yamago, S.; Watanabe, Y.; Iwamoto, T. *Angew. Chem., Int. Ed.* **2010**, *49*, 757−759.
(13) Jasti, R.; Bhattacharjee, J.; Neaton, J. B.; Bertozzi, C. R. *J. Am. Chem. Soc.* **2008**, *130*, 17646−17647.
(14) Kayahara, E.; Patel, V. K.; Yamago, S. *J. Am. Chem. Soc.* **2014**, *136*, 2284−2287.
(15) Evans, P. J.; Darzi, E. R.; Jasti, R. *Nat. Chem.* **2014**, *6*, 404−408.
(16) Xia, J.; Jasti, R. *Angew. Chem., Int. Ed.* **2012**, *51*, 2474−2476.
(17) Kayahara, E.; Iwamoto, T.; Suzuki, T.; Yamago, S. *Chem. Lett.* **2013**, *42*, 621−623.
(18) Xia, J.; Bacon, J. W.; Jasti, R. *Chem. Sci.* **2012**, *3*, 3018−3021.
(19) Yuan, K.; Guo, Y.-J.; Zhao, X. *J. Phys. Chem. C* **2015**, *119*, 5168−5179.
(20) Yuan, K.; Zhou, C.-H.; Zhu, Y.-C.; Zhao, X. *Phys. Chem. Chem. Phys.* **2015**, *17*, 18802−18812.
(21) Fomine, S.; Zolotukhin, M.; Guadarrama, P. *J. Mol. Model.* **2012**, *18*, 4025−4032.
(22) Rehman, H. U.; McKee, N. A.; McKee, M. L. *J. Comput. Chem.* **2016**, *37*, 194−209.
(23) Alvarez, M. P.; Burrezo, P. M.; Kertesz, M.; Iwamoto, T.; Yamago, S.; Xia, J.; Jasti, R.; Navarrete, J. T. L.; Taravillo, M.; Baonza, V. G.; Casado, J. *Angew. Chem., Int. Ed.* **2014**, *53*, 7033−7037.
(24) Kawase, T.; Nishiyama, Y.; Nakamura, T.; Ebi, T.; Matsumoto, K.; Kurata, H.; Oda, M. *Angew. Chem., Int. Ed.* **2007**, *46*, 1086−1088.
(25) Ess, D. H.; Houk, K. N. *J. Am. Chem. Soc.* **2007**, *129*, 10646−10647.
(26) Ess, D. H.; Houk, K. N. *J. Am. Chem. Soc.* **2008**, *130*, 10187−10198.
(27) Frisch, M. J.; et al. *Gaussian 09*, rev. D.01; Gaussian, Inc.: Wallingford CT, 2009.
(28) Chai, J.-D.; Head-Gordon, M. *Phys. Chem. Chem. Phys.* **2008**, *10*, 6615−6620.
(29) Cossi, M.; Rega, N.; Scalmani, G.; Barone, V. *J. Comput. Chem.* **2003**, *24*, 669−681.
(30) Ribeiro, R. F.; Marenich, A. V.; Cramer, C. J.; Truhlar, D. G. *J. Phys. Chem. B* **2011**, *115*, 14556−14562.
(31) Becke, A. D. *J. Chem. Phys.* **1993**, *98*, 5648−5650.
(32) Sure, R.; Grimme, S. *J. Chem. Theory Comput.* **2015**, *11*, 3785−3801.
(33) Marenich, A. V.; Cramer, C. J.; Truhlar, D. G. *J. Phys. Chem. B* **2009**, *113*, 6378−6396.

DOI: 10.1021/acs.joc.6b00339
J. Org. Chem. 2016, 81, 4559−4565